Supplemental Text 1

1. Geochronological method

Measurements from LA-ICP-MS were undertaken in the Central Analytical Facility (CAF) at Stellenbosch University, South Africa; Trace Element and Radiogenic Isotope Laboratory (TRAIL) at the University of Arkansas, USA; whereas ID-TIMS measurements were carried out at the British Geological Survey (BGS), UK; and Berkley Geochronology Center (BGC), USA (see Supplemental Table S1 for all measurements). The MDA calculations based on ID-TIMS are approximately an order of magnitude more precise than those based on LA-ICP-MS due to the well-known lower 2σ analytical uncertainties associated with U-Pb dates acquired via ID-TIMS relative to those acquired via LA-ICP-MS, which are ~0.1% and ~2–3%, respectively (Schaltegger et al., 2015; Horstwood et al., 2016; see Supplemental Table S1). It should be noted that some of the preferred MDAs, which we emphasize that are maximum age constraints, may be affected by Pb-loss. We recognize that this can influence the accuracy of the MDAs, however, we cannot access the potential magnitude of the Pb-loss in the individual samples. The uncertainty of the MDAs is also further increased by the fact that each detrital zircon grain that yielded data for the MDA calculations is associated with sediment reworking of unknow duration prior to its final deposition in the strata of the Elliot and Clarens formations.

1.1 Measurements from LA-ICP-MS

At SU CAF, we used a 193 nm wavelength ASI Resolution laser ablation system coupled to a Thermo Scientific Element 2 single collector magnetic sector field ICPMS. At TRAIL, we used an Elemental Scientific Inc, NWR 193 Excimer laser ablation system coupled to a Thermo-Scientific iCap quadrupole ICP-MS. At BGS, we used a Nu Plasma HR multi-collector ICPMS and at BGC.

Between 30 and 112 detrital zircons were successfully ablated for each sample; Supplemental Table S1 contains a summary of the number of ablated zircons, concordant zircons, concordant zircons younger than 250 Ma, and the distribution of the zircon ages. Data on the detrital zircon standards used for each analytical run at the four analytical facilities involved in this study are shown in last few sheets* of the Supplemental Table S1.

At SU CAF, zircons were hand-picked, embedded in an epoxy mount and polished to expose their midsections for the examination of their internal structure by cathodoluminescence imaging. The laser sampling protocol employed a 30 µm spot and a fluence of 1.4 J/cm^2 (or a 25 µm static spot and a fluence of 2.0 J/cm^2) or a 20 µm spot and a fluence of ~2.0-2.5 J/cm^2, respectively. All samples were ablated for 30 seconds. Geochronological standards (i.e., Plesovice - Sláma et al., 2008; Zircon 95100 - Wiedenbeck et al., 1995; M15 Nasdala et al., 2016 were ablated at regular intervals between sample unknowns to authenticate the validity of the ablation signals in the unknowns.

At TRAIL, zircon grains were mounted on double-sided sticky tape and 150 grains were randomly selected and ablated for 20 seconds using a 25 µm spot size and a repetition rate of 10 Hz with a helium flow rate of 0.8 L/min and fluence of ~4.3 J/cm^2. The primary standard used was Zircon 91500 (1065 Ma; Wiedenbeck et al., 1995) with Plesovice (337.13 Ma; Slama et al., 2008) and R33 (419 Ma; Black et al., 2004) as secondary standards.

1.2 Measurements from CA-TIMS

High precision CA-TIMS dating of selected detrital zircons was performed both at BGS (n=16) and at the BGC (n=12).

At BGS, LA-ICP-MS data were gathered for screening purposes: firstly, grains were mounted on double sided tape and the exterior portion of the grains were analysed, in contrast to conventional LA-ICP-MS where the mid sections of grains are analysed. Although the exterior portions of grains are more susceptible to Pb-loss, the data were of sufficient quality to differentiate Mesozoic grains from Palaeozoic and older. After LA-ICP-MS screening, young detrital zircon factions ($^{206}Pb/^{238}U$ < 250 Ma) were removed and chemically abraded prior to dissolution in order to minimize the effects of Pb-loss (Mattinson, 2005). Based on their external morphology and internal features, only the best zircons were selected for dissolution, which involved multiple steps of acid refluxing, heating and rigorous cleaning. Annealing was carried out at 900˚C for 60 hours, and leaching was done at 180˚C for ~12 hours. Samples were spiked using the gravimetrically calibrated ET535 or ET2535 EARTHTIME U–Pb tracer solutions (Condon et al., 2015; McLean et al., 2015). Isotope ratios were measured on a Thermo-Electron Triton TIMS. Pb was measured in dynamic mode on a MassCom secondary electron multiplier; Pb mass bias corrections were made using a fractionation factor of 0.14 ± 0.02 % amu-1 (1 sigma) for samples spiked using ET535. Dead-time and linearity of the secondary electron multiplier were monitored using repeated analyses of the standards NBS 982, NBS 981 and U 500. U oxide (UO_2) was measured and corrected for isobaric interferences using a $^{18}O/^{16}O$ value of 0.00205 (IUPAC value and measured in-house at the National Isotope Geosciences Laboratories, UK).

At BGC, young detrital zircon crystals from sample LGT (originally named 1455-1) where extracted from the epoxy mount, annealed, chemically abraded and after dissolution analysed using a Micromass Sector 54 Thermal Ionization Mass Spectrometer. Methods follow those described in Mundil et al. (2004). Analytical details for CA-TIMS analyses at BGC are found in Supplemental Table S1. A ^{205}Pb-^{233}U-^{235}U tracer solution mixed and calibrated at BGC was used for all fractions. Calibration of the tracer solution using age solutions and natural standards is documented in Irmis et al. (2011) and Griffis et al. (2018) to facilitate comparison with ET535 derived ages. Bias between the tracer solutions used in this study is within the quoted reproducibility of the BGC tracer (at 0.15%).

1.3 Data reduction

Data reduction was performed using a combination of the software packages Iolite v.3.5 (Paton *et al*., 2011) and VizualAge (Petrus and Kamber, 2012). At TRAIL, analyses were manually adjusted to avoid portions of the analysis that exhibited discordance or ^{204}Pb contamination. At BGS, the algorithms of Schmitz and Schoene (2007) were used for the U-Pb ID-TIMS data reduction. At BGC, U-Pb CA-TIMS data were reduced using an in house data reduction package implemented in Excel, and Isoplot (Ludwig, 2008). For grains with ^{206}Pb/^{238}U age less than 800 Ma concordance was calculated using $\frac{\mathrm{206Pb/238U}}{\mathrm{207Pb/235U}}$ *100 and ^{206}Pb/^{238}U isotopic ratios were interpreted as the dates. For grains with a ^{206}Pb/^{238}U age greater than 800 Ma concordance was calculated using $\frac{\mathrm{206Pb/238U}}{\mathrm{207Pb/206Pb}} * 100$ and ^{207}Pb/^{206}Pb isotopic ratios were interpreted as the dates. A concordance filter of 90-110% was applied and only data that lie within this filter were considered in age interpretations (Supplemental Table S1). The Th/U value of the zircons in each sample, a proxy for their metamorphic (Th/U <0.1) vs igneous (Th/U>0.1) origin (Wu and Zheng, 2004), is also shown in Supplemental Table S1.

1.4 Estimation of the maximum depositional age (MDA)

Multiple metrics for estimating maximum depositional age (MDA) of the samples (see Table 1 in the manuscript) were used for comparison with existing age estimates derived from litho- bio-, ichno- and magnetostratigraphic frameworks (e.g., Kitching and Raath, 1984; Bordy et al., 2004; Bordy and Erikson, 2015; Sciscio et al., 2017; McPhee et al., 2017). Standard metrics outlined in Dickinson and Gehrels (2009) and further discussed in Coutts et al. (2019) are used in this study to estimate the MDA of the samples: (1) the youngest single grain (YSG); (2) the youngest cluster overlapping at 1σ internal error for two or more grains (YC1σ[2+]); (3) the youngest cluster overlapping at 2σ internal error for three or more grains (YC2σ[3+]); and (4) the youngest graphical peak of a probability density plot represented by at least two grains (YPP[2+]). We also used two additional methods: (5) the youngest cluster overlapping at 2σ internal error for two or more grains (YC2σ[2+]) and (6) the concordia age determined by the built-in function of Isoplot 4.15 Software for the youngest detrital zircon grains that overlap at 2σ on the Concordia diagram (Supplemental Table S1, Supplemental Figure S1). Concordance diagrams and plots of the weighted mean dates (at 95% confidence) for zircons < ~250 Ma were generated using Isoplot 4.15 software, and probability density plots (PDPs) for zircons < 500 Ma were produced using the age display MS Excel spreadsheet (Sircombe, 2004; Supplemental Figure S1).

2. Detrital zircon U-Pb geochronology dates: justification of the MDAs and TDAs

This sample-by-sample appraisal is to be read in conjunction with Figures 2, 4 and 5, Table 1, Supplemental Table S1, and Figure S1. In the text below, the maximum depositional age is abbreviated as MDA, whereas the true depositional age is abbreviated as TDA. Our preferred Jurassic MDAs are in blue and preferred Triassic MDAs are in purple. In general, the use of the YSG as an estimation of the MDA is problematic and has been demonstrated that the YSG may be often younger than the TDA (e.g., Anderson et al., 2019; Gehrels et al., 2019; Herriott et al., 2019; Rossingnol et al., 2019). It is therefore preferable to be conservative and select ages that overlap to yield an older MDA. We wish to reiterate that in selecting our preferred MDAs, we adhere to the concept of a maximum depositional age constraint (i.e., we prefer to be conservative by treating our MDAs as maximum constraints on the age of deposition and not as the depositional age). Moreover, it should be noted that the relatively high value of the mean squared weighted deviation (MSWD) in some of the samples (see Figure S1) is expected because of the exclusively detrital nature of the zircons in this study (i.e., our samples are a mixture of grains that were not co-genetic; Horstwood, 2008; Spencer et al., 2016.)

Sample ID	Brief description	Age interpretation
BH-15	Five concordant analyses were obtained from this upper lEF sandstone sample at Bramleys Hoek (Fig. 5). All analyses have Th/U ratios greater than 0.1 (range 0.47 – 1.59). The concordant $^{206}Pb/^{238}U$ dates span from 180.6±0.3 to 217.52±0.23 Ma.	For estimating the MDA of the sample, we considered seven MDA metrics that range between 180.6 and 205 Ma, with six of the metrics yielding dates around ~205 Ma. The youngest zircon dated at 180.6 Ma is discordant indicating Pb-loss (e.g., Corfu, 2013; Anderson et al., 2019; Gehrels et al., 2019; Herriott et al., 2019; Rossingnol et al., 2019), $^{207}Pb/^{206}Pb$ date is 210 ± 5 Ma, which is the best estimate for that crystal. Given the stratigraphic position of the sample and the Toarcian Karoo basalts (Figs. 2, 4), a Rhaetian MDA is geologically more plausible than a Toarcian one. Likewise, based on its YC2σ(2+) date (at 95% confidence), we consider the MDA of BH-15 to be possibly 204.9±0.88 Ma, and TDA not to be younger than late Rhaetian.
GV-14	This lEF sandstone sample from the lower slopes of Mafube (Fig. 5) comprises only two concordant zircon grains with Th/U ratios of 0.53 and 0.70. The	For estimating the MDA of the sample, we considered the age of the younger concordant zircon grain, which is 212.1±0.19 Ma. This estimated late Norian MDA for GV-14 is consistent with other lEF samples in the region (HB-15 and SUB – see Figs. 4, 5

	individual $^{206}Pb/^{238}U$ dates for these two zircon grains are 212.1±0.19 and 220.2±0.26 Ma.	and S1). Moreover, sample GV-14 was taken ~65 m below sample MAF (Fig. 4), which yielded a YC2σ(2+) date of ~201 Ma. We consider the TDA of GV-14 not to be younger than Rhaetian.
HB-15	Fourteen concordant analyses were obtained from this reworked tuffaceous siltstone sample from the lEF at Heelbo (Fig. 5). The concordant $^{206}Pb/^{238}U$ dates range from 216.5±4.7 to 1733±36 Ma, with age peaks at approximately 493, and 520 Ma. The Th/U ratio of the concordant analyses vary between 0.02 and 0.75, with only two analyses having Th/U < 0.1.	For estimating the MDA of the sample, we considered all nine MDA metrics that range between 216.5 and 520 Ma, with three dates being Norian and six being Cambrian. Given the stratigraphic position of the sample, especially relative to the overlying PS-15 sample (Fig. 4), a Norian MDA is geologically more reasonable. Therefore, based on its YC2σ(2+) date, we consider the MDA of HB-15 to be possibly 218.2±2 Ma, and the TDA not to be younger than middle to late Norian.
HAF	Eighty-five concordant analyses were obtained from this medium- to coarse-grained lEF sandstone sample at Quthing (Ha Falatsa; Fig. 5). The Th/U ratios of all analyses are greater than 0.1 (range: 0.14 – 2.19). The $^{206}Pb/^{238}U$ dates vary between 208±3 and 2084±35 Ma, with age peaks at 209, 220, 510 and 1082 Ma.	For estimating the MDA of the sample, we considered all nine MDA metrics, which show a narrow range of 1.5 Ma, from 208.2 to 209.7 Ma. Given the stratigraphic position of sample HAF (Fig. 4) in conjunction with its YC2σ(2+) date (at 95% confidence), we consider the MDA of HAF to be possibly 209.6±1.4 Ma. The TDA of the sample is likely latest Norian to early Rhaetian.
LEP	Eighty-two concordant analyses were obtained from this fine-grained middle uEF sandstone sample at Lephoto. The Th/U ratios are between 0.06 and 2.57 (one analysis of 0.06), and the $^{206}Pb/^{238}U$ concordant dates rage from 196±3 to 3079±39 Ma, with peaks at 196, 243, 251 and 463 Ma.	For estimating the MDA of the sample, we considered all nine MDA metrics that vary between 195.7 and 243 Ma. Of the nine metrics, five yield middle Sinemurian dates between 195.7 and 197.3 Ma. Given the stratigraphic position of sample LEP (Fig. 4), in conjunction with its YC2σ(2+) date, we consider the MDA of LEP to be possibly 197.3±2.3 Ma. The TDA of the sample is likely middle to late Sinemurian.
LGT	Twelve analytically concordant U-Pb zircon CA-TIMS dates were obtained from this reworked tuffaceous siltstone sample from the middle lEF near Lady Grey (Fig. 5). Th/U ratio ranges from 0.87 to 1.56 and $^{206}Pb/^{238}U$ ages range from 196.89±.94 to 212.01±.84 Ma, with the former likely being affected by Pb-loss.	For estimating the MDA of sample LGT, we considered nine MDA metrics that vary between 196.89 and 209.11 Ma. The Sinemurian age (196.89 Ma) of the youngest single zircon is likely because of Pb-loss in that crystal (e.g., Corfu, 2013), and given the problems with YSG dates (see introduction to this section and main text), we disregard this date in the age estimation of the LGT sample. It is also possible that the youngest cluster of 3 crystals (208.01±0.86 Ma) was also affected by Pb-loss as they show excess

		scatter (see Anderson et al., 2019 for a discussion on the possibility of concealed Pb-loss, even within concordant grains). Because the mean $^{206}Pb/^{238}U$ age of the next youngest clearly reproducible cluster of 5 crystals (209.11±0.20; Fig. S1) corresponds more with the local and regional stratigraphic position of this sample (Figs. 4, 5), we consider the most likely MDA for sample LGT to be ~209 Ma (Fig. S1). Our combined evidence suggests that the TDA of the sample is probably not younger than earliest Rhaetian.
LK-17	Twenty-five concordant analyses, four of which have Th/U ratios <0.1, were obtained from this reworked tuffaceous siltstone sample from the upper lEF at Likhoele (Fig. 5). The $^{206}Pb/^{238}U$ dates span from 195.7±5.8 to 1601±51 Ma, with peaks at approximately 207, 484, 520 and 985 Ma.	For estimating the MDA of the sample, we considered all nine MDA metrics that vary between 195.7 and 467 Ma. The Sinemurian age (195.7 Ma) of the youngest single zircon is linked to Pb-loss in that grain (e.g., Corfu, 2013; Anderson et al., 2019; Gehrels et al., 2019; Herriott et al., 2019; Rossignol et al., 2019). Of the nine metrics, six yielded dates of ~207 Ma, which in conjunction with the stratigraphic position of the sample (Fig. 4), point to a Rhaetian MDA. Based on its YC2σ(2+) date (at 95% confidence), we consider the MDA of LK-17 to be possibly 207±5 Ma. The TDA of the sample is likely not younger than middle Rhaetian.
LMO	Sixty-eight concordant analyses were obtained from this fine-medium grained uEF sandstone sample in Quthing (Lower Moyeni; Fig. 5). The Th/U ratios are between 0.1 and 2.04, and the concordant $^{206}Pb/^{238}U$ dates vary between 193.9±9 and 2894±33 Ma, with age peaks at approximately 194, 273, 520, 899 and 1014 Ma.	For estimating the MDA of the sample, we considered all nine MDA metrics that vary between 193.9 to 232 Ma. Given these ages and stratigraphic position of LMO (Fig. 4), a very Early Jurassic MDA is geologically most plausible for this sample. Based on its YC2σ(2+) date (at 95% confidence), we consider the MDA of LMO to be possibly 199.9±2.3 Ma. The TDA of the sample is likely between early and middle Sinemurian.
MAF	Eighty-five concordant analyses were obtained from this fine-medium grained uEF sandstone sample at Mafube (Fig. 5), with Th/U ratios ranging from 0.04 to 2.09 (2 analyses Th/U <0.1). The concordant $^{206}Pb/^{238}U$ dates range between 199.1±3.2 and 2059±26 Ma, with peaks at approximately 256, 464 and 537 Ma.	For estimating the MDA of the sample, we considered eight of the nine MDA metrics that vary between 199.1 and 256.4 Ma. Given these ages and stratigraphic position of MAF (Fig. 4), a very Early Jurassic MDA is geologically most plausible for this sample, especially in the light of the third younger grain of 195±4 Ma in the dataset, which lies outside the 10% discordance filter (11% discordant). Based on its YC2σ(2+) date, we consider the MDA of MAF to be possibly 201±2.3 Ma. The TDA of the sample is likely between early and middle Sinemurian.

MAP	Eighty-two concordant analyses were obtained from this medium-grained middle lEF sandstone sample in Maphutseng (Fig. 5). The Th/U ratios range from 0.12 to 2.83, and the concordant $^{206}Pb/^{238}U$ dates vary between 201±2 and 2791±28, with graphical age peaks at approximately 200 (201, 216, 220), 530 (519,533 and 540) and 1000 (973 and 1046) Ma.	For estimating the MDA of the sample, we considered all nine MDA metrics that range from 201.0 to 215.4 Ma. Seven metrics are congruent at 201 Ma (range from 201.0 and 201.3 Ma), and although these Hettangian dates are most prevalent, a Norian MDA is most likely for MAP, given its stratigraphic position (Fig. 4). Based on its YC2σ(3+) date, we consider the MDA of MAP to be likely 215.4±1.9 Ma, and the TDA not to be younger than late-middle to late Norian.
PHU	One hundred concordant analyses were obtained from this medium-grained lowermost lEF sandstone sample in Puthiatsana (Fig. 5). The Th/U ratios of these concordant analyses range between 0.03 and 1.8, with 4 analyses having Th/U <0.1. The $^{206}Pb/^{238}U$ dates vary from 218±3 to 2898±36 Ma, with peaks at 243, 512, 531, 642 and 1082 Ma.	For estimating the MDA of the sample, we considered all nine MDA metrics that vary from 217.6 to 243.1 Ma. Four of the metrics yield Norian dates that range between 217.6 and 220.0 Ma, and five of the metrics yield Anisian dates (range 242.6 – 243.1 Ma). Given the stratigraphic position of sample PHU (Fig. 4), a Norian age interpretation is geologically more plausible. Based on its YC2σ(2+) date (at 95% confidence), we consider the MDA of SUB to be possibly 219.6±2.5 Ma, and the TDA not to be younger than late-middle to late Norian.
PS-15	Eight concordant analyses were obtained from this middle-upper uEF sandstone sample at Heelbo (Fig. 5). The analyses are all 100% concordant and have Th/U ratios above 0.1 (range: 0.49-0.67). The $^{206}Pb/^{238}U$ dates vary from 202.3±0.19 to 219.7±0.2 Ma, with seven of the eight dates being older than 216 Ma.	For estimating the MDA of the sample, we considered nine MDA metrics that range from 202.3 to 217.2, with eight of the metrics yielding dates of ~217 Ma. Although 217 Ma is the most prevalent date, a Norian MDA is highly unlikely for PS-15, given the stratigraphic position of the sample (Fig. 4), especially its proximity to the Clarens Formation and the body fossils at the PS sample site, which yielded the relatively derived osteological remains of *Pulanesaura* (McPhee et al., 2015). Using the youngest single grain (YSG) metric, the MDA of 202.3±0.19 Ma is assigned for PS-15, however we emphasise that the TDA of PS-15 may be **significantly** younger, probably Hettangian or even early Sinemurian considering the series of ages in 199-197 Ma range of samples LMO and LEP in the lower to middle uEF (e.g., LMO, LEP – see Figs. 4, 5 and S1).
SUB	Ninety-three concordant analyses were obtained from this medium-grained lowermost lEF sandstone sample at Subeng (Leribe; Fig. 5). Note that zircon analysis identifier for this sample is “leribe” in Table	For estimating the MDA of the sample, we considered eight of the nine MDA metrics that range from 215.4 to 252 Ma. Six metrics are congruent with an age range between 215.4 and 216.4 Ma. Given the stratigraphic position of sample SUB (Fig. 4), a Norian MDA is more geologically plausible than a Permian age. Based on its YC2σ(2+)

	S1. The Th/U ratios range from 0.01 to 1.36, with 7 analyses having Th/U ratios < 0.1. The concordant $^{206}Pb/^{238}U$ dates vary from 215±3 to 1610±23 Ma, with age peaks at 216, 252, 525, 535 and 1082 Ma.	date (at 95% confidence), we consider the MDA of SUB to be possibly 216.4±2.4 Ma, and the TDA not to be younger than late-middle to late Norian.
Q6	Fifty-five concordant analyses, three of which have Th/U ratios < 0.1, were retrieved from this medium-grained uppermost uEF sandstone sample (from the base of the Clarens Formation) in Quthing (Hekeng; Fig. 5). The concordant $^{206}Pb/^{238}U$ dates range between 190±2.4 and 1846±15.5 Ma, with age peaks at 193, 256, 468 and 1088 Ma.	For estimating the MDA of the sample, we considered eight of the MDA metrics which vary between 190 and 467.4 Ma. The YC2σ(3+) metric is the only metric considered that does not yield a date between 190 and 193.4 Ma. Given the stratigraphic position of the sample (Fig. 4), in conjunction with its YC2σ(2+) date, we consider the MDA of Q6 to be possibly 191.9±1.5 Ma. The TDA of the sample is likely not younger than latest Sinemurian.
QSS1	Eighty-two concordant analyses, ten of which have Th/U ratios <0.1, were obtained from this medium-grained lower lEF sandstone sample at Driefontein (Fig. 5). The $^{206}Pb/^{238}U$ dates range from 207.5±9 to 2580±41.5 Ma, with age peaks at 213, 529 and 1026 Ma.	For estimating the MDA of the sample, we considered eight of the nine MDA metrics, which show a range from 207.5 to 213 Ma. Given the stratigraphic position of the sample (Fig. 4) in conjunction with its YC2σ(2+) date (at 95% confidence), we consider the MDA of QSS1 to be possibly 211.5±2.8 Ma. The TDA of the sample is probably latest Norian (and less likely early Rhaetian).
UMC	Eighty concordant analyses, one of which has a Th/U ratio <0.1, were obtained from this medium-grained sandstone sample from the uppermost Clarens Formation in Quthing (Upper Moyeni; Fig. 5). The $^{206}Pb/^{238}U$ dates range from 185.9±2.2 to 2056.6±17.3 Ma, with probability density age peaks at 187, 262 and 522 Ma.	For estimating the MDA of the sample, we considered eight of the nine MDA metrics, which are tightly constrained between 185.9 and 187.5 Ma and suggest a Pliensbachian MDA for this sample. Based on its YC2σ(2+) date (at 95% confidence), we consider the MDA of UMC to be possibly 187.5±1.6 Ma. The TDA of the sample is probably middle to late Pliensbachian.

3. Key to the animal silhouettes and ichnites in Figure 2

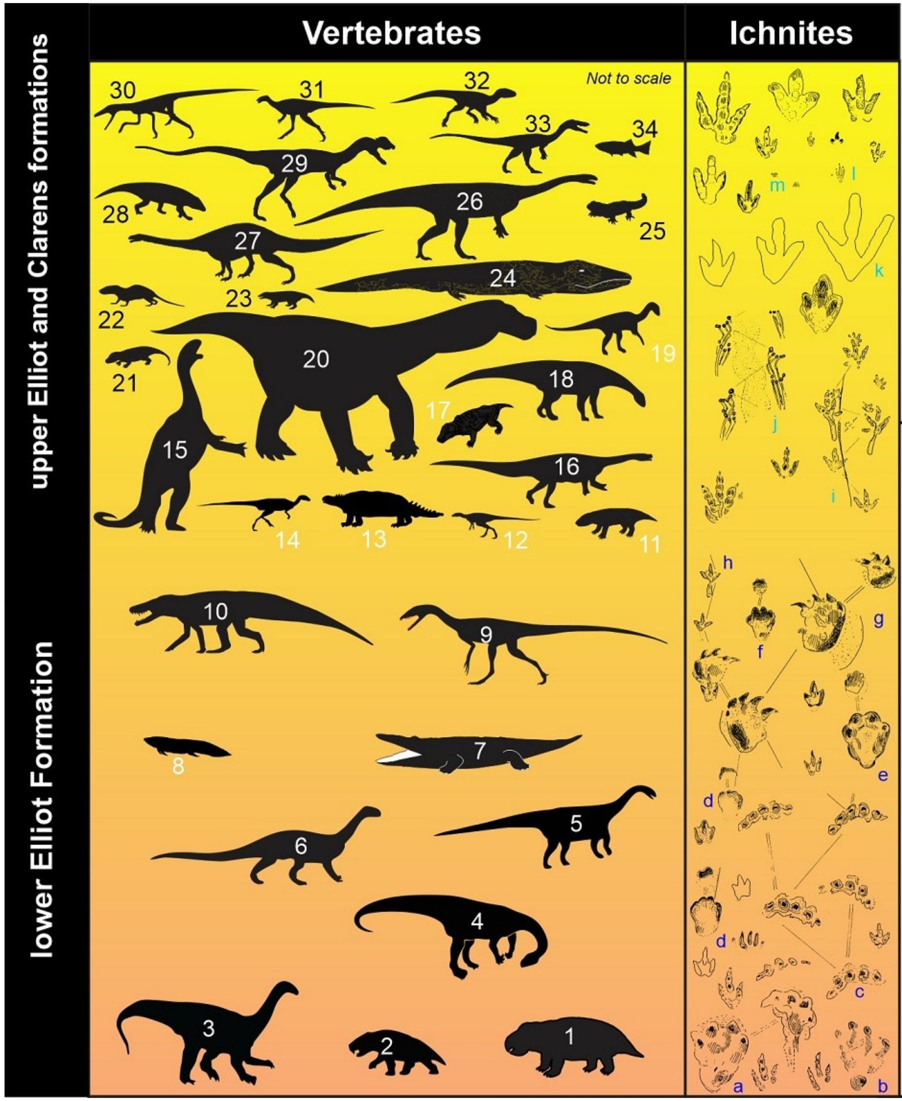

1 - Dicynodontia (*Pentasaur* sp.)
2 - Eucynodontia (*Scalenodontoides* sp.)
3 - Sauropodomorpha (*Blikanasaurus* sp.)
4 - Sauropodomorpha (*Eucnemesaurus* sp.)
5 - Sauropodomorpha (*Melanorosaurus* sp.)
6 - Sauropodomorpha (*Plateosauravus* sp.)
7 - Stereospondyli
8 - *Ceratodus* (lungfish)
9 - Theropoda (teeth only)
10 - Pseudosuchia
11 - Eucynodontia (*Elliotherium* sp.)
12 - Ornithischia (*Eocursor* sp.)
13 - Testudinata (*Australochelys africanus*)
14 - Ornithischia (*Lesothosaurus* sp.)
15 - Sauropodomorpha (*Antetonitrus* sp.)
16 - Sauropodomorpha (*Aardonyx* sp.)
17 - Eucynodontia (*Trithelodon* sp.)
18 - Sauropodomorpha (*Pulanesaura* sp.)
19 - Sauropodomorpha (*Arcusaurus* sp.)
20 - Sauropodomorpha (*Ledumahadi* sp.)
21 - Eucynodontia (*Tritylodon* sp.)
22 - Mammiliaformes (*Megazostrodon* sp.)
23 - Eucynodontia (*Pachygenelu* sp.)
24 - Stereospondyli (*Brachyopoidea* sp.)
25 - Sphenodontia (*Clevosaurus* sp.)

m - tentative cf. *Brasilichnium*-like tracks
l - Kalosauropus
k - Kayentapus ambrokholohali
i - Episcopopus ventrosus
i - Moyenisauropus isp.
h - *Trisauropodiscus* isp.
g - *Tetrasauropus unguiferus*
f - *Sauropodopus antiquus*
e - *Sauropodopus ("Deuterosauropodus major")*
d - *cf. Brachychirotherium ("Deuterosauropodus minor")*
c - *Pentasauropus incredibilis*
b - *Pseudotetrasauropus bipedoida*
a - *?Lavinipes jaquesi*

Unlabeled tridactyl tracks: *Grallator-Eubrontes* plexus ichnites

Source of ichnite outlines: ***Ellenberger 1970***

26 - Sauropodomorpha (*Massospondylus* sp.)
27 - Sauropodomorpha (*Ignavusaurus* sp.)
28 - Crocodylomorpha (*Protosuchus* sp.)
29 - Theropoda (*Dracovenator* sp.)
30 - Crocodylomorpha
31 - Ornithischia
32 - Ornithischia (*Heterodontosaurus* sp.)
33 - Theropoda (*Megapnosaurus* ("*Syntarsus*") *rhodesiensis*)
33 - Pisces (*Semionotus capensis*)

References cited only in this supplementary text (references already cited in the manuscript text are not repeated here)

Condon, D.J., Schoene, B., McLean, N.M., Bowring, S.A. and Parrish, R.R., 2015. Metrology and traceability of U–Pb isotope dilution geochronology (EARTHTIME Tracer Calibration Part I). Geochimica et Cosmochimica Acta, 164, pp.464–480

Griffis, N.P., Mundil, R., Montañez, I.P., Isbell, J., Fedorchuk, N., Vesely F., Iannuzzi, R., and Yin, Q.-Z., 2018. A new stratigraphic framework built on U-Pb single-zircon TIMS ages and implications for the timing of the penultimate icehouse (Paraná Basin, Brazil). GSA Bulletin 130, pp. 848-858.

Horstwood, M., 2008. Data reduction strategies, uncertainty assessment and resolution of LA-(MC-) ICP-MS isotope data. In Sylvester, P.: Laser Ablation ICP-MS in the Earth Sciences: Current Practices and Outstanding Issues. Mineralogical Association of Canada Short Course Series 40, pp. 283 –303.

Horstwood, M.S., Košler, J., Gehrels, G., Jackson, S.E., McLean, N.M., Paton, C., Pearson, N.J., Sircombe, K., Sylvester, P., Vermeesch, P. and Bowring, J.F., 2016. Community-derived standards for LA-ICP-MS U-(Th-) Pb geochronology–Uncertainty propagation, age interpretation and data reporting. Geostandards and Geoanalytical Research, 40(3), pp.311–332.

Irmis, R.B., Mundil, R., Martz, J.W. and Parker, W.G., 2011. High-resolution U–Pb ages from the Upper Triassic Chinle Formation (New Mexico, USA) support a diachronous rise of dinosaurs. Earth and Planetary Science Letters 309, pp. 258-267.

Ludwig, K.R., 2008. User's manual for Isoplot 3.6. Berkeley Geochronology Center, Berkeley, p. 77.

Mundil, R., Ludwig, K.R., Metcalfe, I. and Renne, P.R., 2004. Age and timing of the Permian mass extinctions: U/Pb dating of closed-system zircons. Science 305, pp. 1760-1763.

Nasdala, L., Corfu, F., Valley, J.W., Spicuzza, M.J., Wu, F.Y., Li, Q.L., Yang, Y.H., Fisher, C., Münker, C., Kennedy, A.K. and Reiners, P.W., 2016. Zircon M127–A homogeneous reference material for SIMS U–Pb geochronology combined with hafnium, oxygen and, potentially, lithium isotope analysis. Geostandards and Geoanalytical Research, 40(4), pp.457–475. https://doi.org/10.1111/ggr.12123.

Paton, C., Hellstrom, J., Paul, B., Woodhead, J. and Hergt, J., 2011. Iolite: Freeware for the visualisation and processing of mass spectrometric data. Journal of Analytical Atomic Spectrometry, 26(12), pp.2508–2518. Doi:10.1039/C1JA10172B.

Petrus, J.A. and Kamber, B.S., 2012. VizualAge: A novel approach to laser ablation ICP-MS U-Pb geochronology data reduction. Geostandards and Geoanalytical Research, 36(3), pp.247–270. https://doi.org/10.1111/j.1751-908X.2012.00158.x.

Schaltegger, U., Schmitt, A.K. and Horstwood, M.S.A., 2015. U–Th–Pb zircon geochronology by ID-TIMS, SIMS, and laser ablation ICP-MS: recipes, interpretations, and opportunities. *Chemical Geology*, *402*, pp.89-110.

Schoene, B., Guex, J., Bartolini, A., Schaltegger, U. and Blackburn, T.J., 2010. Correlating the end-Triassic mass extinction and flood basalt volcanism at the 100 ka level. Geology, 38(5), pp.387–390.

Sircombe, K.N., 2004. AgeDisplay: an EXCEL workbook to evaluate and display univariate geochronological data using binned frequency histograms and probability density distributions. Computers & Geosciences, 30(1), pp.21–31.

Sláma, J., Košler, J., Condon, D.J., Crowley, J.L., Gerdes, A., Hanchar, J.M., Horstwood, M.S., Morris, G.A., Nasdala, L., Norberg, N. and Schaltegger, U., 2008. Plešovice zircon—a new natural reference material for U–Pb and Hf isotopic microanalysis. Chemical Geology, 249(1-2), pp.1–35.

Schmitz, M.D. and Schoene, B., 2007. Derivation of isotope ratios, errors, and error correlations for U-Pb geochronology using 205Pb-235U-(233U)-spiked isotope dilution thermal ionization mass spectrometric data. *Geochemistry, Geophysics, Geosystems, 8*, Q08006, doi:10.1029/2006GC001492

Wiedenbeck, M.A.P.C., Alle, P., Corfu, F., Griffin, W.L., Meier, M., Oberli, F.V., Quadt, A.V., Roddick, J.C. and Spiegel, W., 1995. Three natural zircon standards for U-Th-Pb, Lu-Hf, trace element and REE analyses. Geostandards newsletter, 19(1), pp.1–23. https://doi.org/10.1111/j.1751-908X.1995.tb00147.x.

~~Wotzlaw, J.-F., Hüsing, S.K., Hilgen, F.J. and Schaltegger, U., 2014. High-precision zircon U–Pb geochronology of astronomically dated volcanic ash beds from the Mediterranean Miocene. Earth and Planetary Science Letters 407, pp. 19-34. (cited in Supp Table 1)~~